Calculation of the effect of random superfluid density on the temperature dependence of the penetration depth.

Thomas M. Lippman[1,2] and Kathryn A. Moler[1,2,3,*]

[1]*Stanford Institute for Materials and Energy Sciences,*

SLAC National Accelerator Laboratory,

2575 Sand Hill Road, Menlo Park, CA 94025, USA.

[2]*Department of Physics, Stanford University,*

Stanford, California 94305-4045, USA.

[3]*Department of Applied Physics, Stanford University,*

Stanford, California 94305-4045, USA.

(Dated: February 6, 2012)

Abstract

Microscopic variations in composition or structure can lead to nanoscale inhomogeneity in superconducting properties such as the magnetic penetration depth, but measurements of these properties are usually made on longer length scales. We solve a generalized London equation with a non-uniform penetration depth, $\lambda(\boldsymbol{r})$, obtaining an approximate solution for the disorder-averaged Meissner screening. We find that the effective penetration depth is different from the average penetration depth and is sensitive to the details of the disorder. These results indicate the need for caution when interpreting measurements of the penetration depth and its temperature dependence in systems which may be inhomogeneous.

PACS numbers: 74.62.En,74.20.-z,74.62.Dh,74.81.-g

I. INTRODUCTION

The penetration depth and its temperature dependence are important characteristics of any superconductor and are considered key to determining the momentum space structure of the order parameter.[1–3] The possibility of disorder in exotic superconductors is well known, but analyses performed to date have concentrated on the effect of disorder-induced scattering on the momentum space structure of the gap.[4–7] This paper is motivated by the possibility that disorder may lead to nanoscale real space variation and the associated need to model the relationship between such spatial variation and properties that are measured on longer length scales. We address how inhomogeneity in the penetration depth may affect bulk measurements of the penetration depth for methods that rely on Meissner screening and can be analyzed by solutions to London's equation. In particular, we show that the measured result is not simply given by the average value of the penetration depth, but is affected by the statistical structure of the spatial variations in the penetration depth.

Many superconductors are created by chemical doping of a non-superconducting parent compound. In these systems the inherent randomness of the doping process may give rise to an inhomogeneous superconducting state. The importance of this effect will be determined by the characteristic length over which the dopant atoms affect the superconductivity. Even in the most ordered material, there will be binomial fluctuations in the total number of dopants in a given region. In general, one does not expect significant spatial variation in materials that are weakly correlated and can be described by a rigid band model. For example, disorder is largely irrelevant in classic metallic superconductors, due to their long coherence lengths and weakly correlated nature.[8] In contrast, the cuprates are doped insulators with a coherence length on the scale of the lattice. They are known to have nanoscale disorder in their superconducting properties, as seen by scanning tunneling microscopy.[9] Similar gap maps have been observed in the iron pnictide family[10–12] and in disordered titanium nitride films close to the superconductor to insulator transition.[13,14]

Materials with intrinsic disorder present two separate challenges. Understanding how the random doping process gives rise to local superconducting properties, such as the penetration depth or local density of states, requires a microscopic model. But even with such a model, we still need to make the connection between the local superconducting properties and bulk measurements. The manner in which local superconducting properties relate to the observed

2

properties will differ from experiment to experiment. For instance, a measurement of the heat capacity will return the total heat capacity of the macroscopic sample, so the inferred specific heat capacity will be a volume average over the sample. In contrast, we might expect the thermal conductivity response to be dominated by a percolation path connecting regions with small local gap, $\Delta(\boldsymbol{r})$, or large local density of states.

Here we focus on the penetration depth, λ, as measured by screening of the magnetic field, including both resonant cavity frequency shift measurements at radio frequencies[2] and the local probes of Magnetic Force Microscopy[15] and Scanning SQUID Susceptometry.[16] These methods measure $\lambda(T)$ by detecting the response magnetic field generated by the superconductor due to an applied field, and can be analyzed using the London equation. Thus, we can model the effect of inhomogeneity by solving the London equation with $\lambda(\boldsymbol{r})$ as a random function of position $\boldsymbol{r}$. Our goal is to find a new equation for the disorder-averaged magnetic field, as this will determine the measured response. Here, we work in the limit of small fluctuations to find an approximate equation for the disorder-averaged magnetic field, as this will determine the measured response.

II. STOCHASTIC LONDON EQUATION

To understand the measured penetration depth when $\lambda(\boldsymbol{r})$ is a random function of position, we calculate the disorder-averaged magnetic field response to obtain an effective penetration depth. For isotropic and local superconductors in three dimensions, the static magnetic field $h(\boldsymbol{r})$ is given by the London equation with $\lambda(\boldsymbol{r})$ a function of position. The correct form[17] of the London equation when the penetration depth is non-uniform is:

$$\boldsymbol{h} + \boldsymbol{\nabla} \times \left[\lambda(\boldsymbol{r})^2 \, \boldsymbol{\nabla} \times \boldsymbol{h} \right] = 0, \tag{1}$$

which is derived from the second Ginzburg-Landau equation in the London limit.[18] We parametrize the penetration depth as the average value plus a fluctuating term:

$$\lambda(\boldsymbol{r}) = \Lambda \left[1 + \xi(\boldsymbol{r}) \right], \tag{2}$$

so that $\langle \lambda(\boldsymbol{r}) \rangle = \Lambda$. Then Eq. 1 becomes:

$$(L + M_1 + M_2) \, \boldsymbol{h} = 0, \tag{3}$$

where:

$$L \equiv 1 - \Lambda^2 \nabla^2 \boldsymbol{I},$$

$$M_1 \equiv -2\Lambda^2 \xi \nabla^2 \boldsymbol{I} + 2\Lambda^2 \boldsymbol{\nabla} \xi \times \boldsymbol{\nabla} \times, \quad \text{and} \tag{4}$$

$$M_2 \equiv -\Lambda^2 \xi^2 \nabla^2 \boldsymbol{I} + \Lambda^2 \boldsymbol{\nabla} \xi^2 \times \boldsymbol{\nabla} \times.$$

Here $\boldsymbol{I}$ is the identity tensor, and the "dangling curl" is understood to operate on a vector to its right. The terms are grouped so that M_1 is first-order in ξ, M_2 is second-order in ξ, and L gives the unperturbed London equation. We will work in the limit of small fluctuations, $\xi(\boldsymbol{r}) \ll 1$, so that $M_1 + M_2$ is a perturbative term in Eq. 3.

Our method of solution comes from the similarity of the Helmholtz and London equations. The Helmholtz equation, which governs wave propagation, becomes the London equation when the wavevector is purely imaginary. Thus our problem is related to the propagation of waves in a random medium, and we can build upon a large and multidisciplinary literature devoted to this challenge.[19,20] The paper by Karal and Keller[21] is particularly relevant, because it retains the vectorial nature of the problem, rather than simplifying to a scalar wave equation.

We now derive, from Eq. 3, an approximate equation for the disorder-averaged field $\langle \boldsymbol{h} \rangle$. Applying the inverse of L to both sides:

$$\left[1 + L^{-1}(M_1 + M_2) \right] \boldsymbol{h} = \boldsymbol{h}_0, \tag{5}$$

where $L \boldsymbol{h}_0 = 0$. Solving for $\boldsymbol{h}$:

$$\boldsymbol{h} = \left[1 + L^{-1}(M_1 + M_2) \right]^{-1} \boldsymbol{h}_0, \tag{6}$$

assuming the inverse exists. Averaging both sides:

$$\langle \boldsymbol{h} \rangle = \left\langle \left[1 + L^{-1}(M_1 + M_2) \right]^{-1} \right\rangle \boldsymbol{h}_0, \tag{7}$$

where $\boldsymbol{h}_0$ comes outside of the average because it is non-random. Solving for $\boldsymbol{h}_0$:

$$\left\langle \left[1 + L^{-1}(M_1 + M_2) \right]^{-1} \right\rangle^{-1} \langle \boldsymbol{h} \rangle = \boldsymbol{h}_0. \tag{8}$$

Since we assume small fluctuations, we can expand the term inside the average:

$$\left\langle 1 - L^{-1}(M_1 + M_2) + L^{-1}M_1 L^{-1}M_1 + \mathcal{O}(\xi^3) \right\rangle^{-1} \langle \boldsymbol{h} \rangle = \boldsymbol{h}_0. \tag{9}$$

Averaging and expanding again:

$$\left(1 - L^{-1}\langle M_1 L^{-1} M_1\rangle + L^{-1}\langle M_2\rangle\right)\langle \boldsymbol{h}\rangle = \boldsymbol{h}_0, \tag{10}$$

since $\langle M_1\rangle = 0$ due to Eq. 2. We then apply L to both sides:

$$\left(L - \langle M_1 L^{-1} M_1\rangle + \langle M_2\rangle\right)\langle \boldsymbol{h}\rangle = 0, \tag{11}$$

which yields the average field to second order in ξ.

III. RESULTS

We first evaluate the averages in Eq. 11, giving us an equation for $\langle \boldsymbol{h}\rangle$ in terms of the penetration depth correlation function, $\langle \lambda(\boldsymbol{r})\lambda(\boldsymbol{r}')\rangle$. We then consider two specific cases for the correlation function and numerically evaluate the effective penetration depth for a range of parameters.

A. Evaluating the Averages

We will solve Eq. 11 for a single Fourier mode of $\langle \boldsymbol{h}(\boldsymbol{r})\rangle = \boldsymbol{h}\, e^{i\boldsymbol{k}\cdot\boldsymbol{r}}$, then derive an equation for $\boldsymbol{k}$ that yields exponentially decaying solutions consistent with Meissner screening.

First, we evaluate $\langle M_2\rangle$:

$$\langle M_2\rangle = -\Lambda^2\, \langle \xi(\boldsymbol{r})^2\rangle\, \nabla^2 I + \Lambda^2\, \langle \boldsymbol{\nabla}\xi(\boldsymbol{r})^2\rangle \times \boldsymbol{\nabla}\times. \tag{12}$$

We introduce the correlation function $R(\boldsymbol{r}, \boldsymbol{r}') = \langle \xi(\boldsymbol{r})\xi(\boldsymbol{r}')\rangle$, which is a function only of $|\boldsymbol{r}-\boldsymbol{r}'|$ if ξ is stationary and isotropic. Then we see that $\langle \xi^2\rangle = R(0)$ and $\langle \boldsymbol{\nabla}\xi^2\rangle = \boldsymbol{\nabla}\langle \xi^2\rangle = 0$, so

$$\langle M_2\rangle\langle \boldsymbol{h}\rangle = \Lambda^2\, k^2\, R(0)\, \boldsymbol{h}\, e^{i\boldsymbol{k}\cdot\boldsymbol{r}}. \tag{13}$$

We now evaluate the remaining average, $\langle M_1 L^{-1} M_1\rangle$, in three stages to derive Eq. 21. First we expand the differential operations, then evaluate the disorder average. The last stage is to evaluate the integral. We will then combine this integral with Eq. 13 to solve Eq. 11.

The average to evaluate has the form:

$$\langle M_1 L^{-1} M_1\rangle\langle \boldsymbol{h}\rangle = \int d\boldsymbol{r}' \Big\langle M_1(\boldsymbol{r})G(\boldsymbol{r} - \boldsymbol{r}')M_1(\boldsymbol{r}')\Big\rangle\langle \boldsymbol{h}(\boldsymbol{r}')\rangle. \tag{14}$$

5

The Green's function is the solution to $\left(1 - \Lambda^2\nabla^2\right)G(\boldsymbol{r}, \boldsymbol{r}') = \delta(\boldsymbol{r} - \boldsymbol{r}')$, and is:

$$G(z) = \frac{1}{\Lambda^2}\frac{1}{4\pi z}\,e^{-z/\Lambda}. \tag{15}$$

Here, we have defined $\boldsymbol{z} = \boldsymbol{r} - \boldsymbol{r}'$.

We now expand the differential operations in Eq. 14. We do this in two segments, first with derivatives at $\boldsymbol{r}$, then with derivatives at $\boldsymbol{r}'$. The first is:

$$
\begin{aligned}
M_1(\boldsymbol{r})G(\boldsymbol{r} - \boldsymbol{r}')\boldsymbol{v}(\boldsymbol{r}') &= \left[-2\Lambda^2\xi(\boldsymbol{r})\nabla_r^2 + 2\Lambda^2\boldsymbol{\nabla}_r\xi(\boldsymbol{r}) \times \nabla_r\times\right]G(\boldsymbol{r} - \boldsymbol{r}')\boldsymbol{v}(\boldsymbol{r}') \\
&= 2\xi\boldsymbol{v}(\boldsymbol{r}')\big[\delta(\boldsymbol{z}) - G(z)\big] + 2\Lambda^2\boldsymbol{\nabla}\xi \times \big[\nabla_r G(\boldsymbol{r} - \boldsymbol{r}')\big] \times \boldsymbol{v}(\boldsymbol{r}'). \tag{16}
\end{aligned}
$$

The second, which was represented by $\boldsymbol{v}(\boldsymbol{r}')$ above, is:

$$
\begin{aligned}
\boldsymbol{v}(\boldsymbol{r}') = M_1(\boldsymbol{r}')\langle\boldsymbol{h}(\boldsymbol{r}')\rangle &= e^{i\boldsymbol{k}\cdot\boldsymbol{r}'}\Big[2\Lambda^2 k^2\xi(\boldsymbol{r}')\boldsymbol{h} + 2i\Lambda^2\boldsymbol{\nabla}_{r'}\xi(\boldsymbol{r}') \times \boldsymbol{k} \times \boldsymbol{h}\Big] \\
&= 2\Lambda^2 e^{i\boldsymbol{k}\cdot\boldsymbol{r}'}\Big\{\big[k^2\xi(\boldsymbol{r}') - i\,\boldsymbol{\nabla}_{r'}\xi(\boldsymbol{r}') \cdot \boldsymbol{k}\big]\boldsymbol{h} + i\big[\boldsymbol{\nabla}_{r'}\xi(\boldsymbol{r}') \cdot \boldsymbol{h}\big]\boldsymbol{k}\Big\}. \tag{17}
\end{aligned}
$$

Combining Eqns. 16 and 17, we obtain:

$$
\begin{aligned}
M_1(\boldsymbol{r})G(\boldsymbol{r} - \boldsymbol{r}')M_1(\boldsymbol{r}')\langle\boldsymbol{h}(\boldsymbol{r}')\rangle = 2\Lambda^2 e^{i\boldsymbol{k}\cdot\boldsymbol{r}'}\Big\{&\xi(\boldsymbol{r})\xi(\boldsymbol{r}')\big[\delta(\boldsymbol{z}) - G(z)\big]2k^2\boldsymbol{h} \\
&+ \xi(\boldsymbol{r})\boldsymbol{\nabla}_{r'}\xi\big(\boldsymbol{h}\otimes\boldsymbol{k} - \boldsymbol{k}\otimes\boldsymbol{h}\big)2i\big[\delta(\boldsymbol{z}) - G(z)\big] \\
&- 2\Lambda^2 G(z)\big(\Lambda^{-1} + z^{-1}\big)\Big[\xi(\boldsymbol{r}')\boldsymbol{\nabla}_r\xi\big(\boldsymbol{h}\otimes\hat{\boldsymbol{z}} - \hat{\boldsymbol{z}}\otimes\boldsymbol{h}\big)k^2 \\
&+ i\big(\boldsymbol{h}\otimes\hat{\boldsymbol{z}} - \hat{\boldsymbol{z}}\otimes\boldsymbol{h}\big)\big(\boldsymbol{\nabla}_r\xi\otimes\boldsymbol{\nabla}_{r'}\xi\big)\boldsymbol{k} + i\big(\hat{\boldsymbol{z}}\otimes\boldsymbol{k} - \boldsymbol{k}\otimes\hat{\boldsymbol{z}}\big)\big(\boldsymbol{\nabla}_r\xi\otimes\boldsymbol{\nabla}_{r'}\xi\big)\boldsymbol{h}\Big]\Big\}, \tag{18}
\end{aligned}
$$

where we use $\otimes$ to indicate the tensor product.

To perform the disorder average in the second stage, we need various derivatives of the correlation function $R(z)$:

$$
\begin{aligned}
\langle\xi(\boldsymbol{r})\,\boldsymbol{\nabla}_{r'}\xi\rangle &= \boldsymbol{\nabla}_{r'}\,R\big(|\boldsymbol{r} - \boldsymbol{r}'|\big) = -\hat{\boldsymbol{z}}\,\dot{R}(z), \\
\langle\xi(\boldsymbol{r}')\,\boldsymbol{\nabla}_r\xi\rangle &= \boldsymbol{\nabla}_r\,R\big(|\boldsymbol{r} - \boldsymbol{r}'|\big) = \hat{\boldsymbol{z}}\,\dot{R}(z), \quad\text{and} \\
\langle\boldsymbol{\nabla}_r\xi\,\boldsymbol{\nabla}_{r'}\xi\rangle &= \boldsymbol{\nabla}\boldsymbol{\nabla}'\,R(|\boldsymbol{r} - \boldsymbol{r}'|) = -\Big[\frac{\dot{R}}{z}\boldsymbol{I} + \hat{\boldsymbol{z}}\otimes\hat{\boldsymbol{z}}\Big(\ddot{R} - \frac{\dot{R}}{z}\Big)\Big],
\end{aligned}
$$

where the overdot indicates differentiation with respect to z, and $\boldsymbol{I}$ is the identity tensor. Then averaging Eq. 18 gives:

$$
\begin{aligned}
\langle M_1(\boldsymbol{r})G(\boldsymbol{r} - \boldsymbol{r}')M_1(\boldsymbol{r}')\rangle\langle\boldsymbol{h}(\boldsymbol{r}')\rangle = 2\Lambda^2 e^{i\boldsymbol{k}\cdot\boldsymbol{r}'}\Big\{&\big[A(z) + 2k^2 R(z)\delta(z)\big]\boldsymbol{h} \\
&- \big[B(z) + 2i\dot{R}(z)\delta(z)\big]\big(\boldsymbol{k}\otimes\boldsymbol{h} - \boldsymbol{h}\otimes\boldsymbol{k}\big)\hat{\boldsymbol{z}} - C(z)\boldsymbol{h}\big(\hat{\boldsymbol{z}}\otimes\hat{\boldsymbol{z}}\big)\Big\}, \tag{19}
\end{aligned}
$$

with the scalars $A, B,$ and C given by:

$$A(z) = 2k^2 \left[\dot{R}(z)\Lambda^2 G(z)\left(\Lambda^{-1} + z^{-1}\right) - R(z)\, G(z) \right],$$

$$B(z) = 2i \left[\ddot{R}(z)\Lambda^2 G(z)\left(\Lambda^{-1} + z^{-1}\right) - \dot{R}(z)\, G(z) \right], \quad \text{and}$$

$$C(z) = 2\Lambda^2 k^2 \dot{R}(z)\, G(z)\left(\Lambda^{-1} + z^{-1}\right).$$

The final stage in evaluating Eq. 14 is to perform the integral over $\boldsymbol{r'}$. We first change variables from $\boldsymbol{r'}$ to $\boldsymbol{z}$, then integrate over the orientation of $\boldsymbol{z}$. Using the relations

$$\int d\hat{\boldsymbol{z}}\ e^{-i\boldsymbol{k}\cdot\boldsymbol{z}} = 4\pi \frac{\sin(kz)}{kz} \equiv F(k,z),$$

$$\int d\hat{\boldsymbol{z}}\ \hat{\boldsymbol{z}}\, e^{-i\boldsymbol{k}\cdot\boldsymbol{z}} = \hat{\boldsymbol{k}}\, \frac{i}{z}\, \partial_k F, \quad \text{and} \tag{20}$$

$$\int d\hat{\boldsymbol{z}}\ \hat{\boldsymbol{z}} \otimes \hat{\boldsymbol{z}}\, e^{-i\boldsymbol{k}\cdot\boldsymbol{z}} = \frac{-1}{z^2} \left[\frac{\partial_k F}{k} \boldsymbol{I} + \hat{\boldsymbol{k}} \otimes \hat{\boldsymbol{k}} \left(\partial_k^2 F - \frac{\partial_k F}{k} \right) \right],$$

we find that Eq. 14 evaluates to:

$$\int d\boldsymbol{r'} \left\langle M_1(\boldsymbol{r})G(\boldsymbol{r}-\boldsymbol{r'})M_1(\boldsymbol{r'}) \right\rangle \langle \boldsymbol{h}(\boldsymbol{r'}) \rangle = 4\Lambda^2 k^2 e^{i\boldsymbol{k}\cdot\boldsymbol{r}} \left\{ [X + R(0)]\, \boldsymbol{h} + Y\, \hat{\boldsymbol{k}}(\boldsymbol{h}\cdot\hat{\boldsymbol{k}}) \right\}. \tag{21}$$

The functions X and Y are given by:

$$X(k) = \int_0^\infty dz\, G(z) \left\{ \Lambda^2\left(\Lambda^{-1}+z^{-1}\right)\left[\dot{R}\left(z^2 F + k^{-1}\partial_k F\right) - \ddot{R}zk^{-1}\partial_k F \right] + \dot{R}zk^{-1}\partial_k F - Rz^2 F \right\},$$

$$Y(k) = \int_0^\infty dz\, G(z) \left\{ \Lambda^2\left(\Lambda^{-1} + z^{-1}\right)\left[\ddot{R}zk^{-1}\partial_k F + \dot{R}\left(\partial_k^2 F - k^{-1}\partial_k F\right) \right] - \dot{R}zk^{-1}\partial_k F \right\}. \tag{22}$$

We require the average magnetic field to have $\boldsymbol{\nabla}\cdot\boldsymbol{h} = 0$, which means that $\boldsymbol{k}\cdot\boldsymbol{h} = 0$. We now collect our results from Eqns. 21 and 13, and insert them into Eq. 11:

$$\boldsymbol{h}\, e^{i\boldsymbol{k}\cdot\boldsymbol{r}} \left[1 + \Lambda^2 k^2 \left(1 - 3\,R(0) - 4\,X\right) \right] = 0. \tag{23}$$

We are interested in solutions consistent with Meissner screening, so we require that k be positive and purely imaginary. Then the field decays on a length scale $\lambda_{\text{eff}} = \frac{i}{k}$, which we identify as the experimentally measured penetration depth. To calculate λ_{eff}, we will solve the equation:

$$\frac{\lambda_{\text{eff}}^2}{\Lambda^2} = 1 - 3R(0) - 4X. \tag{24}$$

Inserting $k = \frac{i}{\lambda_{\text{eff}}}$ into our equation for X, we get:

$$X = 4\pi \int_0^\infty \mathrm{d}z\, G(z)\sinh\left(\frac{z}{\lambda_{\text{eff}}}\right)\left\{\Lambda^2\left(\Lambda^{-1}+z^{-1}\right)\left[\dot{R}\lambda_{\text{eff}}\, z^{-1}\left(z^2+\lambda_{\text{eff}}^2\right)-\ddot{R}\lambda_{\text{eff}}^3\right]+\dot{R}\lambda_{\text{eff}}^3-Rz\lambda_{\text{eff}}\right\}$$
$$+ 4\pi \int_0^\infty \mathrm{d}z\, G(z)\cosh\left(\frac{z}{\lambda_{\text{eff}}}\right)\left\{\Lambda^2\left(\Lambda^{-1}+z^{-1}\right)\left[-\dot{R}\lambda_{\text{eff}}^2+\ddot{R}z\lambda_{\text{eff}}^2\right]-\dot{R}z\lambda_{\text{eff}}^2\right\}. \quad (25)$$

Valid solutions for λ_{eff} will require the integral for X to converge and Eq. 24 to have solutions.

B. Correlation Function

A full solution of the disorder-averaged magnetic field, $\langle \boldsymbol{h} \rangle$, requires knowledge of the correlation function $R(z)$ and hence requires not only a detailed knowledge of the composition, structure, and disorder of the sample, but also a microscopic model to locally determine the superconducting properties from that structure. Without guidance from microscopic calculations, we will use the Matérn one-parameter family of correlation functions[22] to tune the smoothness, as well as the magnitude and correlation length, of the penetration depth fluctuations. Handcock and Wallis[23] parametrize the Matérn class of covariance functions as:

$$R(z) = \frac{R(0)}{2^{\nu-1}\Gamma(\nu)} \left(2\sqrt{\nu}\,\frac{z}{l}\right)^\nu K_\nu\left(2\sqrt{\nu}\,\frac{z}{l}\right), \quad (26)$$

where K_ν is a modified Bessel function of the second kind and $\Gamma(z)$ is the Gamma function. The intercept at zero separation is the normalized variance of the penetration depth, $R(0) = \sigma_\lambda^2/\langle\lambda\rangle^2 = (\langle\lambda^2\rangle - \langle\lambda\rangle^2)/\langle\lambda\rangle^2$, and quantifies the magnitude of the inhomogeneity in $\lambda(\boldsymbol{r})$. The correlation length, l, controls the size of the fluctuations in $\lambda(\boldsymbol{r})$. The parameter ν controls the smoothness of $\lambda(\boldsymbol{r})$. Larger ν gives a smoother random field, since it is $\lceil\nu\rceil - 1$ times mean squared differentiable, where $\lceil\cdot\rceil$ is the ceiling function.[23]

Two members of the family deserve specific mention. When $\nu = 1/2$, Eq. 26 reduces to the exponential correlation function, $R(z) = R(0)\exp\left(-z\sqrt{2}/l\right)$, which is the correlation function of a Markov process in one dimension. The integrals for X in Eq. 25 diverge when $R(z) \propto e^{-z}$, making the case $\nu = 1/2$ invalid. In the limit where $\nu \to \infty$, $R(z) \to R(0)\exp(-z^2/l^2)$, which is labeled the squared exponential correlation function, to prevent confusion with the Gaussian probability distribution. This correlation function gives the smoothest possible $\lambda(\boldsymbol{r})$ that can be described within the Matérn covariance family.

C. Squared Exponential Correlations

We now consider the case of squared exponential correlations, $R(z) = R(0) \, e^{-z^2/l^2}$. In Fig. 1 we plot four realizations of a normally distributed penetration depth with squared exponential correlations, illustrating the effect of the two parameters l and $R(0)$ on $\lambda(\boldsymbol{r})$. Evaluating Eq. 25 gives:

$$X = -R(0) \int_0^\infty \mathrm{d}z \; e^{-z/\Lambda} e^{-z^2/l^2} \sinh\left(\frac{z}{\lambda_{\mathrm{eff}}}\right) \frac{\lambda_{\mathrm{eff}}}{\Lambda^2} \left[\left(1 + 2\tfrac{\Lambda^2}{l^2}\right) + 2\,z\,\frac{\Lambda}{l^2}\right] \left(1 + 2\tfrac{\lambda_{\mathrm{eff}}^2}{l^2}\right)$$
$$+ 2\,R(0) \int_0^\infty \mathrm{d}z \; e^{-z/\Lambda} e^{-z^2/2l^2} \cosh\left(\frac{z}{\lambda_{\mathrm{eff}}}\right) \frac{\lambda_{\mathrm{eff}}^2}{\Lambda^2} \left[z\,\frac{1}{l^2}\left(1 + 2\tfrac{\Lambda^2}{l^2}\right) + 2\,z^2\,\frac{\Lambda}{l^4}\right]. \quad (27)$$

All of these integrals converge, so we evaluate X as:

$$X = R(0)\frac{2\lambda_{\mathrm{eff}}^2}{l^2}$$
$$+ R(0) \frac{\lambda_{\mathrm{eff}}\sqrt{\pi}}{4l^3\Lambda^2} \left\{ \left(l^4 - 2l^2\Lambda\lambda_{\mathrm{eff}} + 4\Lambda^2\lambda_{\mathrm{eff}}^2\right) \exp\left[\frac{l^2}{4}\left(\frac{1}{\Lambda} + \frac{1}{\lambda_{\mathrm{eff}}}\right)^2\right] \mathrm{erfc}\left[\frac{l}{2}\left(\frac{1}{\Lambda} + \frac{1}{\lambda_{\mathrm{eff}}}\right)\right] \right.$$
$$\left. - \left(l^4 + 2l^2\Lambda\lambda_{\mathrm{eff}} + 4\Lambda^2\lambda_{\mathrm{eff}}^2\right) \exp\left[\frac{l^2}{4}\left(\frac{1}{\Lambda} - \frac{1}{\lambda_{\mathrm{eff}}}\right)^2\right] \mathrm{erfc}\left[\frac{l}{2}\left(\frac{1}{\Lambda} - \frac{1}{\lambda_{\mathrm{eff}}}\right)\right] \right\}. \quad (28)$$

After inserting Eq. 28 into Eq. 24, we solve for λ_{eff} over three decades in the correlation length, l, and in the disorder variance, $R(0)$ (Fig. 2). At large correlation length the effective penetration depth is larger than the average value, representing *suppressed* Meissner screening. Conversely, at small correlation length the effective penetration depth is smaller than the average, indicating *enhanced* screening. The separatrix, where $\lambda_{\mathrm{eff}} = \Lambda$ for all values of $R(0)$, occurs near $l = 1.643\Lambda$. Note that the system is not symmetric about the separatrix, although it becomes more symmetric as $R(0) \to 1$. This is true for both linear and logarithmic spacing around the separatrix. In other words, neither $|\lambda_{\mathrm{eff}}(l_s + \Delta l) - \langle\lambda\rangle| = |\lambda_{\mathrm{eff}}(l_s - \Delta l) - \langle\lambda\rangle|$ nor $|\lambda_{\mathrm{eff}}(al_s) - \langle\lambda\rangle| = |\lambda_{\mathrm{eff}}(l_s/a) - \langle\lambda\rangle|$ are true, where l_s denotes the separatrix, and a is an arbitrary positive real number. As expected, $\lambda_{\mathrm{eff}} \to \Lambda$ as $R(0) \to 0$. Yet even at small disorder, λ_{eff} has variations on the one percent scale, shown by the contours in Fig. 2. As we will discuss below, sub-percent variations of λ_{eff} could be significant in the context of a typical measurement of $\Delta\lambda(T)$.

The trends in λ_{eff} can also be seen in Fig. 3, where we plot $\lambda_{\mathrm{eff}}/\Lambda$ vs. $R(0)$ at fixed correlation length. All three curves taper to $\lambda_{\mathrm{eff}} = \Lambda$ as the magnitude of disorder decreases. At large correlation length, in this case $l = 10\Lambda$, λ_{eff} increases by ten percent when $R(0) =$

0.02. The effect at small correlation is more modest, but still reaches nearly ten percent by the time $R(0) = 0.1$ when $l = 0.1\Lambda$.

The penetration depth has a temperature dependence that it inherits from the underlying disordered superconducting state. It is natural to expect that $R(0)$ and l will have a temperature dependence of their own, which will create a temperature-induced change in λ_{eff}. This change contributes to any measurement of $\lambda(T)$, but is not related to the gap structure in momentum space, because it arises from the spatial arrangement of the superconducting state. If we neglected the spatial variation of λ we would erroneously attribute the entire temperature dependence to the order parameter.

D.   General Matérn Correlations

To understand the impact of the smoothness of $\lambda(\boldsymbol{r})$ on the measured penetration depth, λ_{eff}, we now consider the general case of Matérn covariance. Recall that the parameter ν controls the smoothness of the penetration depth. With the correlation function defined by Eq. 26, we evaluate Eq. 25:

$$
\begin{aligned}
X = & -\frac{R(0)}{2^{\nu-1}\Gamma(\nu)} \int_0^\infty \mathrm{d}z\, e^{-z/\Lambda} \sinh\left(\frac{z}{\lambda_{\text{eff}}}\right) \frac{\lambda_{\text{eff}}}{\Lambda^2 l^4} \left[l^4 \left(2\sqrt{\nu}\frac{z}{l}\right)^\nu K_\nu\left(2\sqrt{\nu}\frac{z}{l}\right) \right. \\
& + 4\nu l^2 \left(\Lambda^2 + \Lambda z + \lambda_{\text{eff}}^2\right) \left(2\sqrt{\nu}\frac{z}{l}\right)^{\nu-1} K_{\nu-1}\left(2\sqrt{\nu}\frac{z}{l}\right) \\
& \left. + 16\nu^2 \lambda_{\text{eff}}^2 \Lambda(\Lambda + z) \left(2\sqrt{\nu}\frac{z}{l}\right)^{\nu-2} K_{\nu-2}\left(2\sqrt{\nu}\frac{z}{l}\right) \right] \\
& + \frac{R(0)}{2^{\nu-1}\Gamma(\nu)} \int_0^\infty \mathrm{d}z\, e^{-z/\Lambda} \cosh\left(\frac{z}{\lambda_{\text{eff}}}\right) \frac{4\nu\lambda_{\text{eff}}^2}{\Lambda^2 l^4} \left[l^2 z \left(2\sqrt{\nu}\frac{z}{l}\right)^{\nu-1} K_{\nu-1}\left(2\sqrt{\nu}\frac{z}{l}\right) \right. \\
& \left. + 4\nu\Lambda(\Lambda + z)z \left(2\sqrt{\nu}\frac{z}{l}\right)^{\nu-2} K_{\nu-2}\left(2\sqrt{\nu}\frac{z}{l}\right) \right]. \quad (29)
\end{aligned}
$$

These integrals can be evaluated using equation 6.621.3 in Gradshteyn and Ryzhik:[24]

$$
\int_0^\infty x^{\mu-1} e^{-\alpha x} K_\nu(\beta x)\mathrm{d}x =
$$

$$
\sqrt{\pi}\frac{(2\beta)^\nu}{(\alpha+\beta)^{\mu+\nu}} \frac{\Gamma(\mu+\nu)\Gamma(\mu-\nu)}{\Gamma(\mu+\frac{1}{2})} {}_2F_1\left(\mu+\nu, \nu+\tfrac{1}{2}; \mu+\tfrac{1}{2}; \frac{\alpha-\beta}{\alpha+\beta}\right), \quad (30)
$$

which requires $\operatorname{Re}\mu > |\operatorname{Re}\nu|$ and $\operatorname{Re}(\alpha + \beta) > 0$. The function ${}_2F_1(a, b; c; z)$ is Gauss' hypergeometric function. Using the integral in Eq. 30 to evaluate Eq. 29, we find the

constraints

$$\nu > \frac{3}{2} \quad \text{and} \quad \frac{\lambda_{\text{eff}}}{\Lambda} > \frac{l}{l + 2\Lambda\sqrt{\nu}}. \tag{31}$$

The full solution for X is then:

$$X = \frac{R(0)\sqrt{\pi}}{\Gamma(\nu)} \left(\frac{4\nu}{l^2}\right)^{\nu} \frac{\lambda_{\text{eff}}}{\Lambda} \left\{ \frac{\lambda_{\text{eff}}^2 + \Lambda^2}{2\Lambda} \frac{\Gamma(2\nu - 1)}{\Gamma(\nu + \frac{1}{2})} \left[a^{-(2\nu-1)} F1(\square) - b^{-(2\nu-1)} F1(\clubsuit)\right] \right.$$

$$+ \frac{\Gamma(2\nu)}{\Gamma(\nu + \frac{3}{2})} \left[\frac{\lambda_{\text{eff}} + \Lambda}{2\Lambda} a^{-2\nu} F2(\square) + \frac{\lambda_{\text{eff}} - \Lambda}{2\Lambda} b^{-2\nu} F2(\clubsuit)\right]$$

$$+ \frac{1}{\Lambda} \frac{\Gamma(2\nu + 1)}{\Gamma(\nu + \frac{3}{2})} \left[a^{-(2\nu+1)} F3(\square) - b^{-(2\nu+1)} F3(\clubsuit)\right]$$

$$+ \frac{\lambda_{\text{eff}}^2 \Lambda}{4} \frac{\Gamma(2\nu - 3)}{\Gamma(\nu - 1)} \left[a^{-(2\nu-3)} F4(\square) - b^{-(2\nu-3)} F4(\clubsuit)\right]$$

$$+ \frac{\lambda_{\text{eff}}}{4} \frac{\Gamma(2\nu - 2)}{\Gamma(\nu + \frac{1}{2})} \left[\left(\lambda_{\text{eff}} + \Lambda\right) a^{-(2\nu-2)} F5(\square) - \left(\lambda_{\text{eff}} - \Lambda\right) b^{-(2\nu-2)} F5(\clubsuit)\right]$$

$$\left. + \frac{\lambda_{\text{eff}}}{2} \frac{\Gamma(2\nu - 1)}{\Gamma(\nu + \frac{3}{2})} \left[a^{-(2\nu-1)} F6(\square) + b^{-(2\nu-1)} F6(\clubsuit)\right] \right\}, \tag{32}$$

where we have introduced the variables

$$a = \frac{1}{\Lambda} + \frac{1}{\lambda_{\text{eff}}} + \frac{2\sqrt{\nu}}{l},$$

$$b = \frac{1}{\Lambda} - \frac{1}{\lambda_{\text{eff}}} + \frac{2\sqrt{\nu}}{l},$$

$$\square = \frac{l(\lambda_{\text{eff}} + \Lambda) - 2\lambda_{\text{eff}}\Lambda\sqrt{\nu}}{l(\lambda_{\text{eff}} + \Lambda) + 2\lambda_{\text{eff}}\Lambda\sqrt{\nu}},$$

$$\clubsuit = \frac{l(\Lambda - \lambda_{\text{eff}}) + 2\lambda_{\text{eff}}\Lambda\sqrt{\nu}}{l(\Lambda - \lambda_{\text{eff}}) - 2\lambda_{\text{eff}}\Lambda\sqrt{\nu}},$$

and functions

$$F1(\cdot) = {}_2F_1(2\nu - 1, \nu - \tfrac{1}{2}; \nu + \tfrac{1}{2}; \cdot),$$

$$F2(\cdot) = {}_2F_1(2\nu, \nu - \tfrac{1}{2}; \nu + \tfrac{3}{2}; \cdot),$$

$$F3(\cdot) = {}_2F_1(2\nu + 1, \nu + \tfrac{1}{2}; \nu + \tfrac{3}{2}; \cdot),$$

$$F4(\cdot) = {}_2F_1(2\nu - 3, \nu - \tfrac{3}{2}; \nu - \tfrac{1}{2}; \cdot),$$

$$F5(\cdot) = {}_2F_1(2\nu - 2, \nu - \tfrac{3}{2}; \nu + \tfrac{1}{2}; \cdot), \quad \text{and}$$

$$F6(\cdot) = {}_2F_1(2\nu - 1, \nu - \tfrac{3}{2}; \nu + \tfrac{3}{2}; \cdot).$$

Inserting this expression for X into Eq. 24, we can solve for λ_{eff} after choosing a value for the smoothness parameter ν. In Fig. 4, we have chosen $\nu = 2$, close to the lower bound

11

of $\frac{3}{2}$ required for convergence of X. The results are almost identical to the case of squared exponential correlations (Fig. 2); evidently λ_{eff} is not much affected by changes in the smoothness of $\lambda(\boldsymbol{r})$ for the Matérn family of correlation functions. The qualitative features of interest to us are still present: there are regions of enhanced screening and regions of suppressed screening, the effect grows on increasing the variance of $\lambda(\boldsymbol{r})$, and changes in λ_{eff} at the one percent level persist down to small disorder. Quantitatively, the results in Figures 4 and 2 differ by five percent in the region near $l = 1$ and $R(0) = 1$, where the difference is largest.

IV. DISCUSSION

The measured $\lambda(T)$ in a non-uniform superconductor will be determined by both the momentum space gap structure and the real space variations of the penetration depth. We calculate the influence of spatial fluctuations in the penetration depth by solving the stochastic London equation in the limit of small fluctuations. This gives an equation (Eq. 24) for the disorder-averaged magnetic field in terms of the penetration depth correlation function. We then solve this equation for two example correlation functions to find λ_{eff}, the decay length of the disorder-averaged field, which we identify as the penetration depth measured experimentally. We find that λ_{eff} can be either smaller or larger than the average penetration depth, depending on the correlation length of λ. More importantly, the variance and correlation length of λ will likely change with temperature, endowing the experimentally measured penetration depth with temperature dependence that is unrelated to the superconducting order parameter.

This work shows that there can be a disorder-induced change of the penetration depth that is not caused by the structure of the superconducting gap in momentum space. Rather, it reflects the real space variations of the order parameter. An interpretation that assumed a spatially uniform penetration depth would infer a larger modulation of $\Delta(\boldsymbol{k})$ than truly exists. Because $\Delta(\boldsymbol{k})$ is the starting point for investigations of the mechanism of the superconductor, this omission could lead us astray when we seek to determine the underlying mechanism.

How significant is the effect of disorder-induced change in the penetration depth, given that $\lambda_{\text{eff}}/\langle\lambda\rangle$ approaches 1 over a large segment of the $R(0)$-l plane? Modern measurements

can routinely resolve sub-nanometer changes in the penetration depth;[1,2,15] in cuprates and pnictides the penetration depth is approximately 200 nm, and a 1-nm change in λ yields $\frac{\Delta\lambda}{\lambda}$ of 0.5% – making even small changes in $\lambda_{\mathrm{eff}}/\langle\lambda\rangle$ potentially significant.

Two issues are worth emphasizing. First, we have made no assumption about the distribution of $\lambda(\boldsymbol{r})$, i.e., whether it is normally distributed or follows a different probability distribution. However, the calculation presented here only extends to second order, and any non-normality only enters at third order and above. Second, λ_{eff} has a complicated dependence on the correlation function $R(z)$, and we know neither its functional form nor its temperature dependence. Hence we cannot make any tidy prediction for the low-temperature behavior of $\lambda(T)$; there is no power-law to be had.

Even without perfect knowledge of $R(z)$, it may be possible learn more about λ_{eff} by taking advantage of the general constraints that apply to all correlation functions.[22,25] In particular, the strong similarities between the two cases presented here (Figs. 2 and 4) lead us to expect qualitatively similar behavior in λ_{eff} for most possible correlation functions.

To make a stronger statement about $\lambda(T)$, we need to determine the local superconducting properties of a given chemically doped and intrinsically disordered material, which naturally depends on the microscopic details of the superconducting mechanism. Although it should be possible to extract a local penetration depth or superfluid density from numerical methods such as solving the Bogoliubov-de Gennes equations on a lattice, to the best of our knowledge this has never been attempted. Several groups have calculated the *disorder-averaged* superfluid stiffness using this approach, for both s-wave[26] and d-wave[27,28] models. The full temperature dependence of the disorder-averaged superfluid density can also be calculated,[29] but is incomplete, for we have shown that the real space inhomogeneity of the superconducting state also contributes to the temperature dependence.

The larger message is that some measured properties of disordered superconductors will not be determined by their disorder averages alone; inhomogeneities can affect the measured properties in an experiment-dependent manner. For example, the heat capacity will be given by the disorder average because it is additive, but we have seen that the penetration depth is non-trivially affected by the disorder. Nonetheless, these two experiments are both traditionally interpreted as measuring the same thing – the magnitude of the single-particle gap, $\Delta(\boldsymbol{k})$.

These results give a specific example of the potential impact of spatial variation on mea-

surements of the penetration depth. With a full consideration of the impact of spatial variation on different measured quantities, as well as a complete understanding of how random chemical doping gives rise to a non-uniform superconducting state, we will be able to integrate a complete account of the effects of disorder into our understanding of unconventional superconductivity.

ACKNOWLEDGMENTS

* kmoler@stanford.edu

[1] W. N. Hardy, D. A. Bonn, D. C. Morgan, R. Liang, and K. Zhang, Physical Review Letters **70**, 3999 (1993).

[2] R. Prozorov and R. W. Giannetta, Superconductor Science and Technology **19**, R41 (2006).

[3] W. N. Hardy, S. Kamal, and D. A. Bonn, in *The Gap Symmetry and Fluctuations in High-Tc Superconductors*, Vol. 371, edited by J. Bok, G. Deutscher, D. Pavuna, and S. A. Wolf (Kluwer Academic Publishers, Boston, 2002) pp. 373–402.

[4] J. Annett, N. Goldenfeld, and S. R. Renn, Physical Review B **43**, 2778 (1991).

[5] V. Mishra, G. Boyd, S. Graser, T. Maier, P. J. Hirschfeld, and D. J. Scalapino, Physical Review B **79**, 094512 (2009).

[6] P. J. Hirschfeld and N. Goldenfeld, Physical Review B **48**, 4219 (1993).

[7] A. B. Vorontsov, M. G. Vavilov, and A. V. Chubukov, Physical Review B **79**, 140507 (2009).

[8] P. G. de Gennes, *Superconductivity Of Metals And Alloys* (Westview Press, 1999).

[9] Ø. Fischer, M. Kugler, I. Maggio-Aprile, C. Berthod, and C. Renner, Reviews of Modern Physics **79**, 353 (2007).

[10] Y. Yin, M. Zech, T. L. Williams, X. F. Wang, G. Wu, X. H. Chen, and J. E. Hoffman, Physical Review Letters **102**, 097002 (2009).

[11] M. L. Teague, G. K. Drayna, G. P. Lockhart, P. Cheng, B. Shen, H. Wen, and N. Yeh, Physical Review Letters **106**, 087004 (2011).

[12] Y. Fasano, I. Maggio-Aprile, N. D. Zhigadlo, S. Katrych, J. Karpinski, and Ø. Fischer, Physical Review Letters **105**, 167005 (2010).

[13] B. Sacépé, T. Dubouchet, C. Chapelier, M. Sanquer, M. Ovadia, D. Shahar, M. Feigel'man, and L. Ioffe, Nat Phys **7**, 239 (2011).

[14] B. Sacépé, C. Chapelier, T. I. Baturina, V. M. Vinokur, M. R. Baklanov, and M. Sanquer, Physical Review Letters **101**, 157006 (2008).

[15] L. Luan, T. M. Lippman, C. W. Hicks, J. A. Bert, O. M. Auslaender, J. Chu, J. G. Analytis, I. R. Fisher, and K. A. Moler, Physical Review Letters **106**, 067001 (2011).

[16] C. W. Hicks, T. M. Lippman, M. E. Huber, J. G. Analytis, J. Chu, A. S. Erickson, I. R. Fisher, and K. A. Moler, Physical Review Letters **103**, 127003 (2009).

[17] J. R. Cave and J. E. Evetts, Journal of Low Temperature Physics **63**, 35 (1986).

[18] The familiar relation $\boldsymbol{J} = -\boldsymbol{A}/\lambda^2$ is not valid when the order parameter is non-uniform. Instead, we start with the Ginzburg-Landau equations, which can describe a non-uniform superconducting state. From the second Ginzburg-Landau equation we derive our starting point, Equation 1, a generalized London equation.

[19] L. A. Mysak, Reviews of Geophysics **16**, 233 (1978).

[20] N. G. Van Kampen, Physics Reports **24**, 171 (1976).

[21] F. C. Karal and J. B. Keller, Journal of Mathematical Physics **5**, 537 (1964).

[22] B. Matérn, *Spatial Variation*, 2nd ed., Lecture Notes in Statistics, Vol. 36 (Springer-Verlag, Berlin, 1986).

[23] M. S. Handcock and J. R. Wallis, Journal of the American Statistical Association **89**, 368 (1994).

[24] I. S. Gradshteyn and I. M. Ryzhik, *Table of Integrals, Series, and Products*, Corrected and Enlarged Edition. (Academic Press, 1980).

[25] N. A. C. Cressie, *Statistics for Spatial Data*, Wiley Series in Probability and Mathematical Statistics. (Wiley, New York, 1991).

[26] A. Ghosal, M. Randeria, and N. Trivedi, Physical Review B **65**, 014501 (2001).

[27] M. Franz, C. Kallin, A. J. Berlinsky, and M. I. Salkola, Physical Review B **56**, 7882 (1997).

[28] A. Ghosal, M. Randeria, and N. Trivedi, Physical Review B **63**, 020505 (2000).

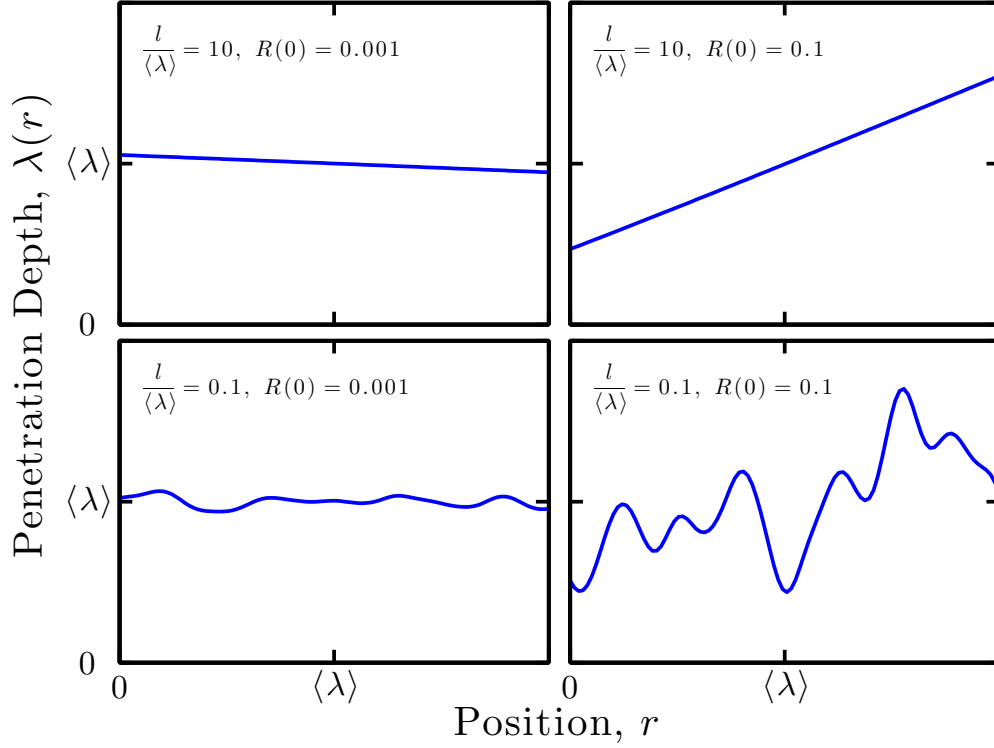[29] T. Das, J.-X. Zhu, and M. J. Graf, arXiv:1105.5109 (2011).

FIG. 1. Sample realizations of a random penetration depth reveal the influence of the correlation length, l, and variance, $R(0)$. The variance, $R(0) = \langle\lambda^2\rangle/\langle\lambda\rangle^2 - 1$, controls the width the penetration depth distribution, and the correlation length establishes the characteristic length over which $\lambda(\boldsymbol{r})$ changes.
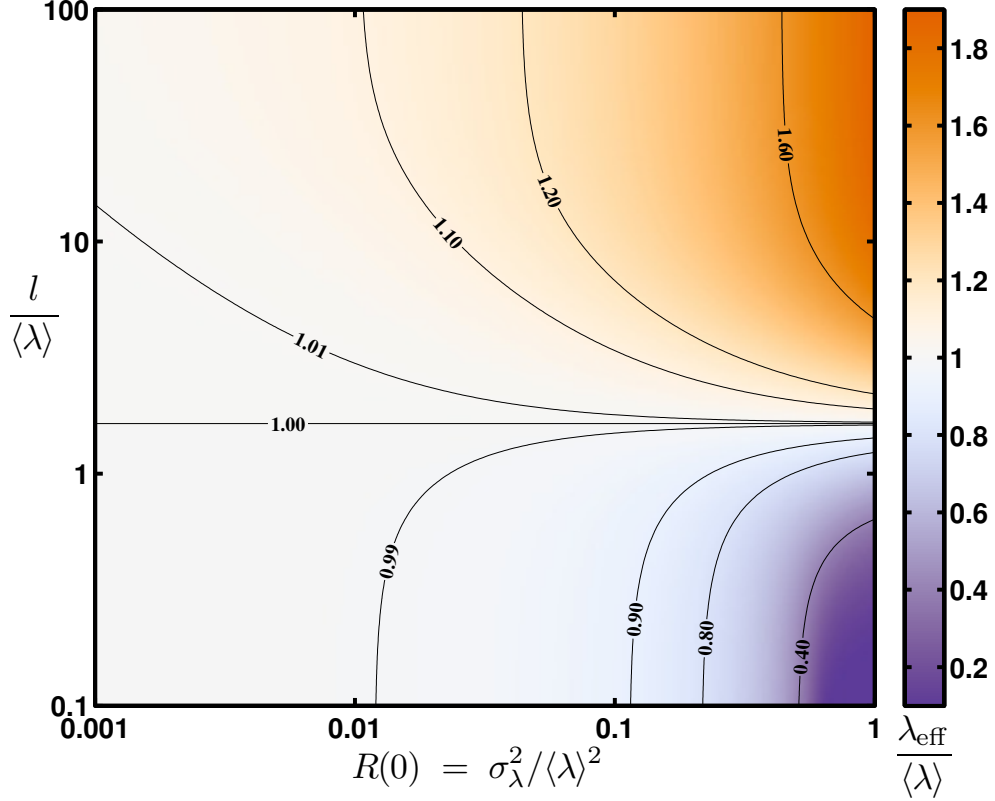
FIG. 2. The effective penetration depth is a strong function of the parameters that characterize the distribution of local penetration depths. Here we show the value of λ_{eff} as the correlation length, l, and variance, $R(0)$, run across three orders of magnitude. This figure considers the case of squared exponential correlations in the penetration depth; a different case is shown in Fig. 4. The most important features of this color plot are the range of $\lambda_{\text{eff}}/\langle\lambda\rangle$ and the appearance of values both above and below 1. The calculation is valid when $R(0) \ll 1$, but we show the region with $R(0) > 0.1$ to emphasize the trends seen. Any temperature dependence in l or $R(0)$ will contribute to $\lambda(T)$. This temperature dependence is not accounted for by the superconducting gap.
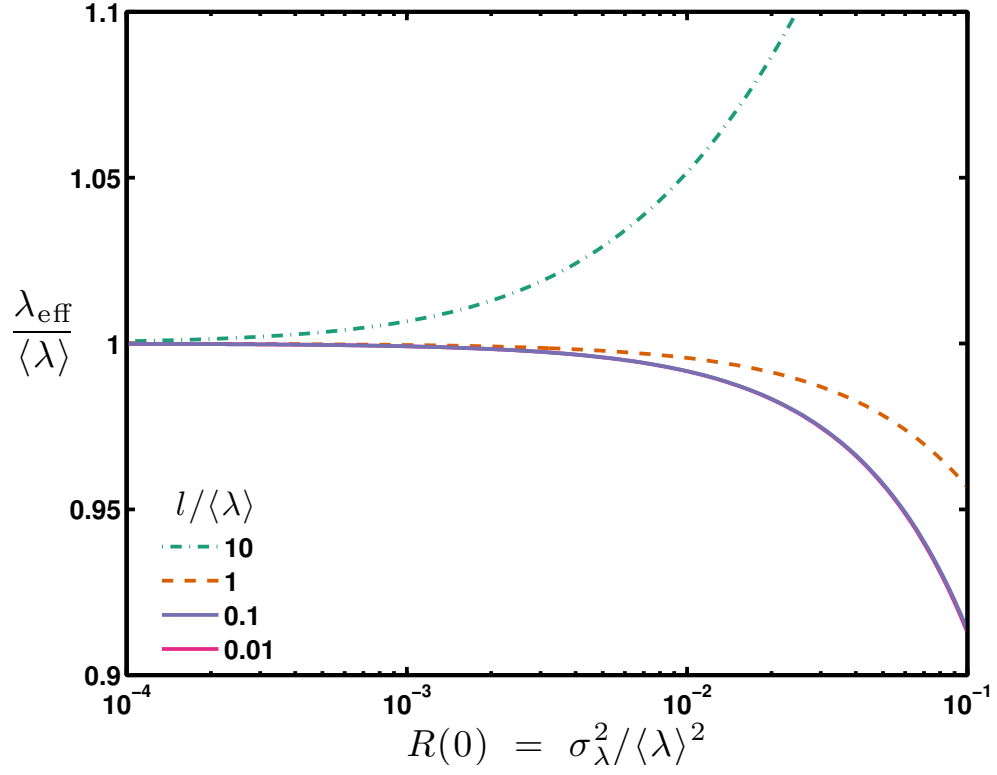
FIG. 3. The screening can either be enhanced ($\lambda_{\text{eff}} < \langle\lambda\rangle$) or suppressed ($\lambda_{\text{eff}} > \langle\lambda\rangle$), depending on the correlation length. The curves for $l = 0.1\langle\lambda\rangle$ and $l = 0.01\langle\lambda\rangle$ overlap.
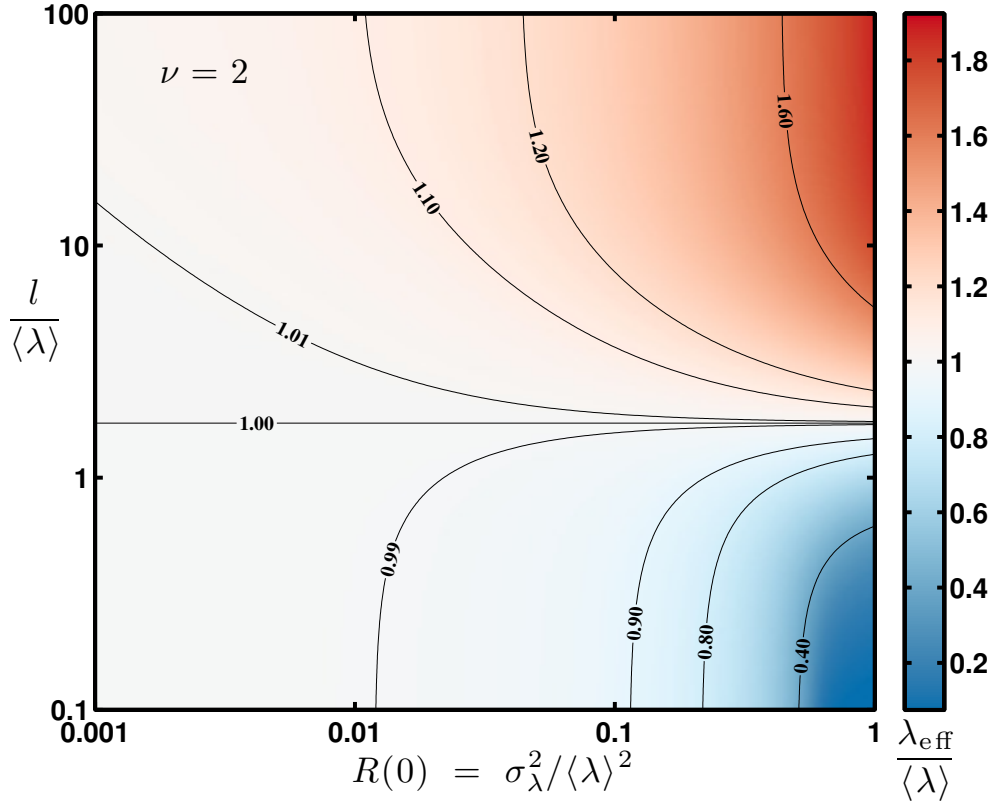
FIG. 4. The effective penetration depth for Matérn correlations when $\nu = 2$ (shown here) has strong similarities to Fig. 2, which represents the limiting case where $\nu \to \infty$. These similarities imply that the smoothness of the random penetration depth does not strongly affect λ_{eff}.